# Fabrication and Characterization of MEMS-Based Resonant Organic Gas Sensors

Arash Hajjam, *Student Member, IEEE*, and Siavash Pourkamali, *Member, IEEE*

***Abstract*— Polymer coated thermal-piezoresistive micromechanical resonant silicon nanobalances have been utilized for detection and concentration measurement of volatile organic compounds in gas phase. Polyglycolic acid, which is the main polymer ingredient of the shipley-1813 photoresist, was used as the absorbent coating layer. Experiments have shown that polymer thickness determines the achievable sensitivity towards the gas molecules. The main challenge is to coat the devices with a thick layer of polymer while still maintaining their high-Q resonance. Multiple polymer coating approaches have been demonstrated. Following polymer deposition, in order to find the sensitivity of the devices, they were tested by exposure to regular gasoline and toluene vapor. The best measurement results were obtained by utilizing the photoresist already present on the resonant structures from the fabrication process. A maximum frequency shift of 3600 ppm (55 kHz) was obtained from a 15.5 MHz resonator with a ~1.5 μm thick coating upon exposure to nitrogen saturated with toluene vapor at room temperature. Based on the measurement results, minimum detectable concentration of toluene in the gas phase for such devices is in the range of a few ppm.**

***Index Terms*— Gas sensing, microelectromechanical systems (MEMS) resonator, micro-resonator, nanobalance, piezoresistive readout, resonant sensor, thermal actuation, volatile organic compound.**

## I. Introduction

HIGHLY sensitive and low-cost organic gas sensors have a number of applications mainly in the oil and gas industry. Examples include early detection of gas leaks and rapid on-site determination of organic content of oil sands. Achieving a high level of selectivity and specificity between different volatile organic compounds (VOC) could be a challenging chemical design issue. However, in most of the targeted applications in oil and gas industry the composition of the compound(s) of interest is somewhat known and constant and the information of interest is their concentration in surrounding air. Most carbon-based polymers have a tendency to absorb organic molecules in the gas phase. Coating a microscale resonator with such polymers will turn the device into a mass balance responding to the concentration of surrounding gas molecules.

Manuscript received October 22, 2011; revised November 30, 2011; accepted December 16, 2011. Date of publication December 22, 2011; date of current version April 25, 2012. The associate editor coordinating the review of this paper and approving it for publication was Prof. Gerald Gerlach.

The authors are with the Department of Electrical and Computer Engineering, University of Denver, Denver, CO 80210 USA (e-mail:ahajjam@du.edu; spourkam@du.edu).

Color versions of one or more of the figures in this paper are available online at http://ieeexplore.ieee.org.

Digital Object Identifier 10.1109/JSEN.2011.2181360

Most of the VOC sensors demonstrated in the literature are based on either conductivity change in a thin film, or resonance frequency change in a mechanical resonator. Conductivity based sensors utilize carbon nanotubes [1, 2] or conductive polymers [3, 4]. Sensing based on resonant frequency shift generally provides more precision as the effect of noise in direct voltage or current measurement is highly suppressed in frequency measurements. A variety of VOC sensors using surface acoustic wave (SAW) [5, 6], quartz crystal microbalance (QCM) [7, 8], and micro electromechanical (MEMS) resonators [9-14] have previously been demonstrated. The miniaturized MEMS resonators can be batch fabricated as individual devices or arrays at a very low cost and due to their much smaller size, they can provide orders of magnitude higher sensitivity and resolution compared to bulky quartz [7, 8] and SAW [5, 6] resonators. Electrostatic (capacitive) MEMS resonant chemical/gas sensors [9-11], some of which are integrated within a CMOS process [10, 11] have previously been demonstrated. For such devices deposition of the chemically sensitive layer used for the detection of VOC is performed by dispensing, spray coating, or drop coating. One of the potential bottle necks for this type of device could be the penetration of the polymer coating inside the air-gaps of the resonator. The polymer residues could cause the air-gaps to clog up and therefore degrade the performance of this type of resonant sensor and even leave them non-operational. Piezoelectric MEMS resonators have also been used for gas sensing purposes through which mass sensitivities in the order of hundred picograms equivalent to minimum detectable gas concentration of few ppm has been achieved [12, 13].

Thermally actuated resonators, as the third group of MEMS resonant sensors, are extremely simple to implement without fabrication challenges or the need for integration of different materials as needed for piezoelectric resonators. The simple monolithic structure of thermal-piezoresistive resonators makes them very robust for sensory applications where the resonator needs to be in contact with the surrounding environment [14,15]. Another major advantage of silicon thermal piezoresistive resonators is that if designed properly and biased with a large enough DC bias current, the internal interactions between the thermal forces and the piezoresistivity of its actuators can lead to self-sustained vibrations without the need for a sustaining amplifier [16]. This makes implementation of sensor arrays using such resonators very convenient. This work presents high frequency versions of such devices capable of detection and concentration measurement of VOC in gas phase.

1530–437X/$26.00 © 2011 IEEE

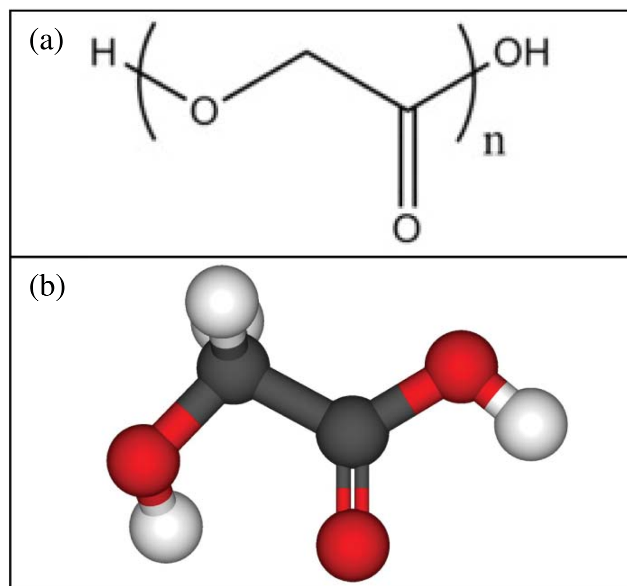


Fig. 1. (a) 2-D and (b) 3-D schematics of the compound structure of polyglycolic acid which is the main polymer ingredient of the shipley-1813 photoresist that was used as the absorbent coating layer.

The resonators in this work are coated with the shipley-1813 photoresist whose main polymer ingredient is polyglycolic acid. Figure 1 shows both the two-dimensional and three-dimensional structure of this non-conductive polymer which is both biodegradable and thermoplastic in nature [17].

## II. Fabrication and Coating Process

The standard single mask silicon on insulator (SOI) MEMS process was used for fabrication of the thermal-piezoresistive resonators used in this work [15]. This process starts by growing a thin (~200 nm) layer of silicon dioxide on the substrate. The silicon dioxide layer is patterned to define the resonator structures. The silicon structures are then carved into the SOI device layer by deep reactive ion etching (DRIE) of silicon all the way down to the buried oxide (BOX) layer. Finally, the underlying buried oxide is removed in hydrofluoric acid (HF). At the same time the remaining oxide mask on top of the structures is also etched away. The whole procedure is shown in steps a to c of Figure 2.

In multiple studies, in order to examine the ability of high frequency crystalline silicon thermal-piezoresistive resonators as VOC sensors, the devices were coated using three different techniques: 1) coating the devices after release from the buried oxide layer (BOX) layer [18], 2) coating the devices before release [19], and 3) using the polymer already present from the fabrication stage [20] to collect the gas molecules. All three methods used the shipley-1813 photoresist as the absorbent coating layer and underwent the same procedure for experimentation.

Each of the sensors were exposed to either gasoline or toluene (the main component of gasoline) vapor. The frequency shift caused by the absorption of the gas vapor was measured using the network analyzer.

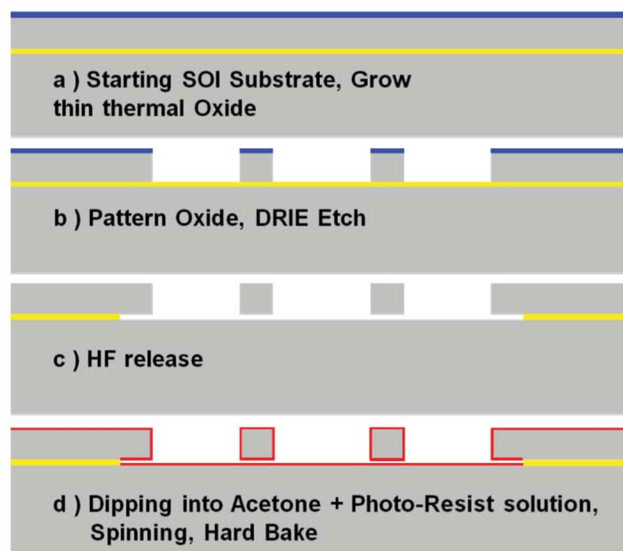


Fig. 2. (a–c) Thermally actuated resonator fabrication process flow and (d) polymer coating.

### A. Polymer Coating After Releasing of the Structures

In the first polymer coating approach, the absorbent polymer layer was formed on the resonators sensing pads by dipping them in a dilute solution of the shipley-1813 photoresist in acetone [18]. The resonator samples were spun at 3000 rpm for a few seconds to disperse the excess diluted photoresist followed by hard bake in order to get rid of the solvent (step d of Figure 2). This is expected to leave a thin dry layer of polymer on all silicon surfaces.

Even though the resonators prepared using this method were responding to organic gases, the sensitivity and full-range frequency shift was not very promising and a maximum frequency shift of only 200 ppm was obtained for a highly saturated gas sample. The reason for such low frequency shift was the small polymer thickness on the surface of the devices due to use of a highly diluted polymer solution. Using higher concentration polymer solutions in this technique, generally results in excessive polymer residues in the gap between the resonators and the SOI handle layer leaving the devices non-operational as can be seen in the SEM picture in Figure 3.

### B. Polymer Coating Before Releasing of the Structures

In order to prevent the resonant devices becoming non-operational due to the forming of the residues in the gap between the SOI handle layer and the resonator, a new procedure was utilized for polymer coating of the devices. Using this coating method, a thicker polymer coating was also obtained as shown in Fig. 4. Steps a and b which are not shown in Fig. 4 are identical to the fabrication process shown in Figure 2. However, in this approach the polymer solution (a much higher concentration solution) is added and spin coated at a speed of 3000 rpm before the devices are undercut [18]. Undercut is done in hydrofluoric acid after coating with polymer (steps c and d of the fabrication process

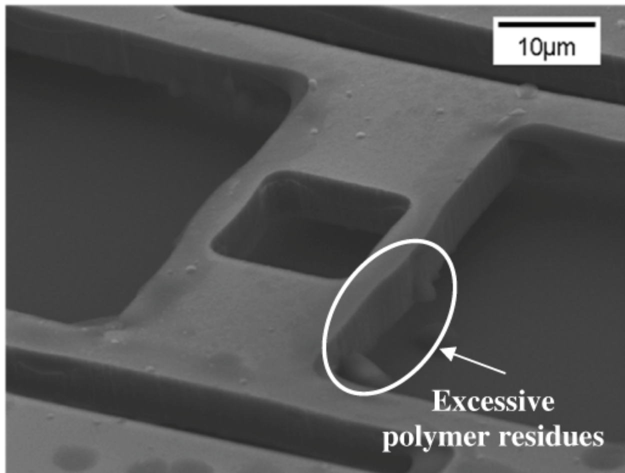


Fig. 3. SEM view of a device in which high polymer thickness has resulted in excessive polymer residues in the gap between the resonators and the SOI handle layer which has left the devices non-operational.

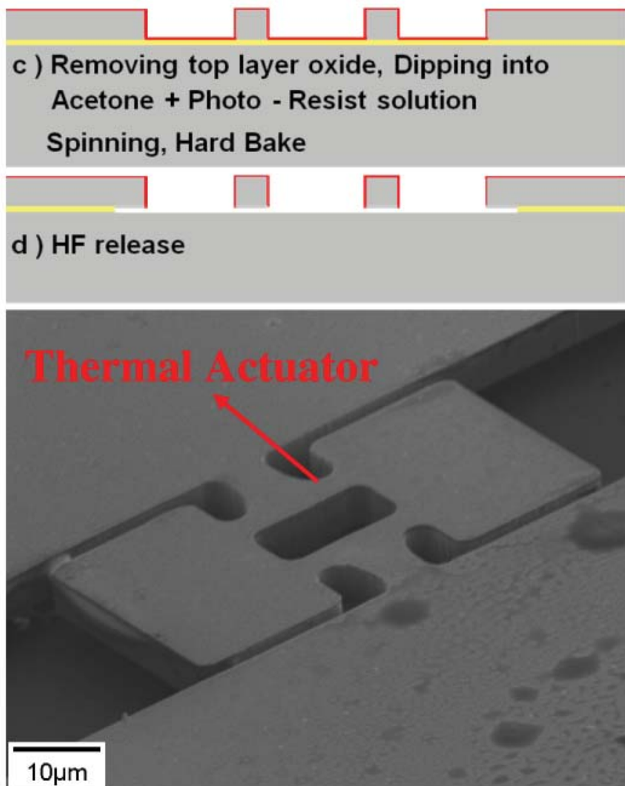


Fig. 4. Second procedure for coating of the thermally actuated resonators in which the polymer is added before the devices are undercut and undercut is done in hydrofluoric acid after coating with polymer. Also, an SEM picture of a 24 MHz I-shaped resonator used for gas sensing and coated using the second method is shown.

shown in Fig. 4). Using this approach there will be no polymer residue underneath the device structures.

SEM view of a 24 MHz I-shaped resonator polymer coated using the abovementioned technique is also shown in Fig. 4. This resonator has been fabricated on a SOI substrate with both device layer and BOX thickness of 5$\mu$m. This coating method showed a 10x improvement in the sensor frequency

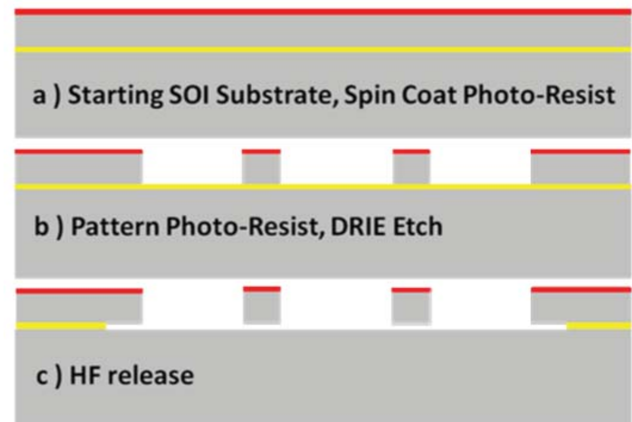


Fig. 5. Thermally actuated resonator fabrication process flow, in which the photoresist used for the patterning is left on the structure as organic absorbent film. There was no initial oxidation in this fabrication approach and the photoresist which forms the coating layer of the resonators was used as the mask. (a) Starting SOI substrate, spin coat photo-resist. (b) Pattern photo-resist, DRIE etch. (c) HF release.

response and higher frequency shifts in the 2200 ppm range were achieved.

Although no polymer residues are to be seen underneath the device structures, there are non-uniform residues on the sidewalls and that limits the use of thicker polymer coatings. Such non-uniformities in the deposited mass could also cause a mass imbalance in the resonant structures causing lower quality factors or leaving the devices non-operational.

### *C. Utilizing the Photoresist Used for Patterning of the Devices as the Absorbent Polymer Coating*

Although the second coating method presented major improvements in the sensor response, getting a thick uniform polymer coating was still a challenge and this fabrication technique suffered from a low process yield. In the third coating technique, the same layer of photoresist used for patterning of the devices, was used as the absorbent layer. For this purpose, as shown in Figure 5, the silicon structures were released in hydrofluoric acid (HF) after carving the structures into the SOI device layer (deep reactive ion etching) without removing the remaining photoresist used as a mask during silicon etch [20]. It should be noted that there was no initial oxidation in this fabrication approach and the photoresist which forms the coating layer of the resonators was used as the mask. Figure 6 shows the SEM view of a released polymer coated 15.5MHz resonator. Although HF has damaged and penetrated through the photoresist at various locations on the wirebond pads next to the resonator, the smaller resonator surfaces were able to tolerate the resulting stress quite well and remain intact.

Using this approach the coating covers the resonator upper surface very uniformly without leaving behind any residues on the resonator sidewalls or in the gap between the resonant structure and the handle substrate. This fabrication method has allowed $\sim$1.5$\mu$m thick polymer coatings to be formed on the surface of the resonator. This has led to higher sensitivities

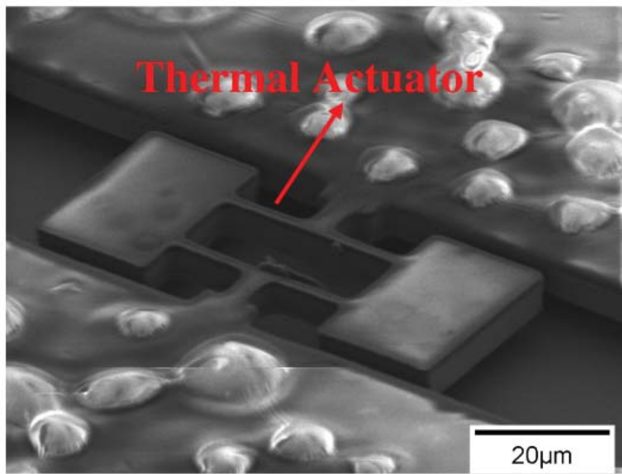


Fig. 6. SEM picture of a 15.5 MHz I-shaped resonator used as gas sensor and polymer coated using the third mentioned method. The actuating beams are 36-$\mu$m long and 3-$\mu$m wide. The two sensing platforms have a dimension of 31 by 22 $\mu$m.

and saturation frequencies in comparison to previous results. Another major advantage associated with this coating procedure is the fact that there are no additional processes required in order to coat the devices.

## III. Resonator Description and Operation

The resonators utilized in this work are referred to as I-Shaped resonators [21-23]. The schematic view of a thermally actuated I-shaped resonator is shown in Figure 7a. Such devices are very suitable for thermal actuation as they can easily be actuated by passing a fluctuating electrical current between the two pads on their two sides. This results in an AC ohmic loss component in the current path. Due to their higher resistance, most of the ohmic loss occurs in the thin pillars located in the middle of the structure. The AC force generated in the pillars as a result of the fluctuating temperature and therefore alternating thermal stress in the pillars, can actuate the resonator in its in-plane resonant mode. The electrical connections and components required for isolation of the AC actuation current from the DC bias current required for operation of the resonator are also shown in Figure 7a. Figure 7b shows the in-plane extensional resonant mode of an I-shaped resonator. In this mode the masses on the two ends of the pillars vibrate back and forth in opposite directions. At resonance, the resistance of the pillars will be modulated by the resulting alternating mechanical stress due to the piezoresistive effect that results in a detectable small signal motional current in the device.

## IV. Measurement Setup and Results

Figure 8 shows the schematic diagram of the setup used to characterize the sensory response of the coated resonators. In this setup, nitrogen bubbled through a liquid gasoline/toluene container is directed towards the resonator under test. Having a flow of the gas sample passing over the resonator surfaces maximizes the contact between potential molecules of interest

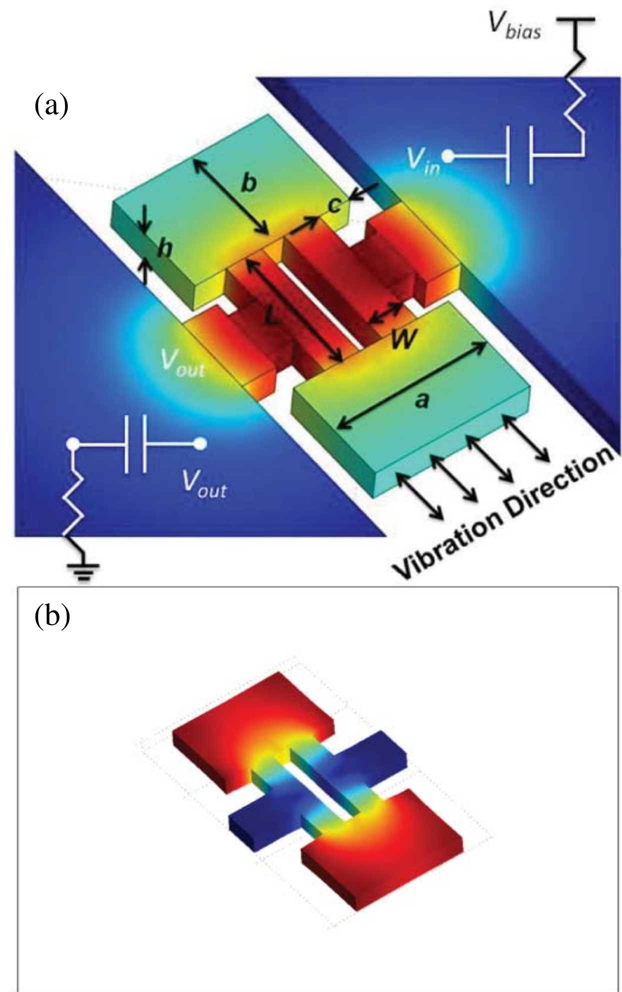


Fig. 7. (a) Schematic view of a thermally actuated I-shaped resonator showing the qualitative distribution of temperature fluctuation amplitude. The electrical connections required for operation of the resonator are also shown. (b) COMSOL eigen frequency analysis results, showing the fundamental in-plane resonance mode shape for a thermally actuated I-shaped resonator. Red and blue colors show locations with the largest and smallest vibration amplitudes respectively.

in the gas sample and the resonator surface, hence, maximizing the absorption probability.

Figure 9 shows the change in the measured frequency versus time for a resonator fabricated using the first approach. The change in frequency was recorded as the device was being exposed to nitrogen flow rich with gasoline vapor at room temperature.

As can be seen, upon exposure, the resonance frequency reduces over time with a time constant of ~4min. Restoration of the resonant frequency to its initial value happens rather quickly as soon as the source is removed. A relatively small maximum frequency shift of only ~200ppm was achieved [18] which is believed to be due to the thin polymer layer used as the absorbent layer and therefore it was decided to turn to other alternative approaches for coating of the devices.

Figure 10 shows the change in the measured frequency versus time for the resonator shown in Fig. 4 which was

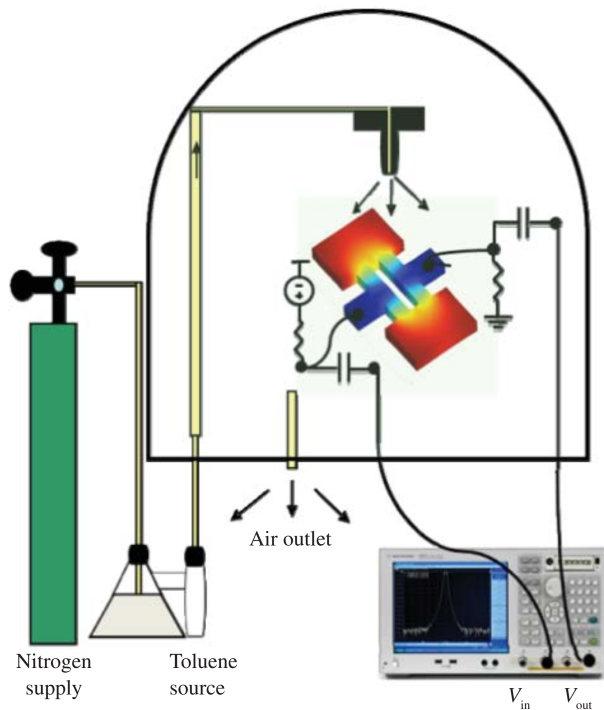


Fig. 8. Schematic diagram of the setup used in order to characterize the resonator sensory response. Here nitrogen bubbled through a toluene Container is directed towards the resonator under test.

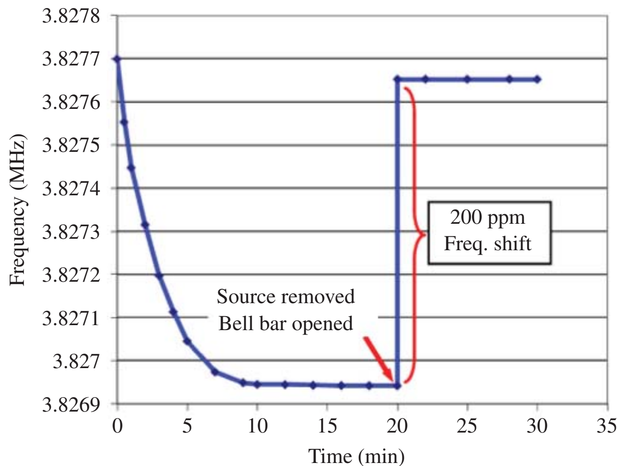


Fig. 9. Change in the measured resonance frequency as a function of the cumulative exposure time for a 3.8 MHz resonator fabricated using the first approach. An overall frequency shift of ~760 Hz (198 ppm) is achieved. The gasoline source was removed after 20 min. The return to a frequency close to the initial frequency happens very quickly.

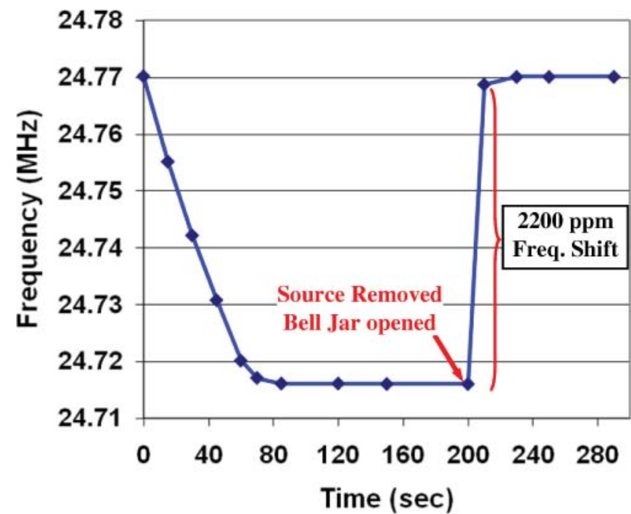


Fig. 10. Change in the measured resonance frequency for the 24 MHz I-shaped resonator of Fig. 4 as a function of the cumulative exposure time showing an overall frequency shift of 54 kHz (2200 ppm). The source was removed after 200 sec. The return to a frequency very close to the initial frequency is almost instantaneous.

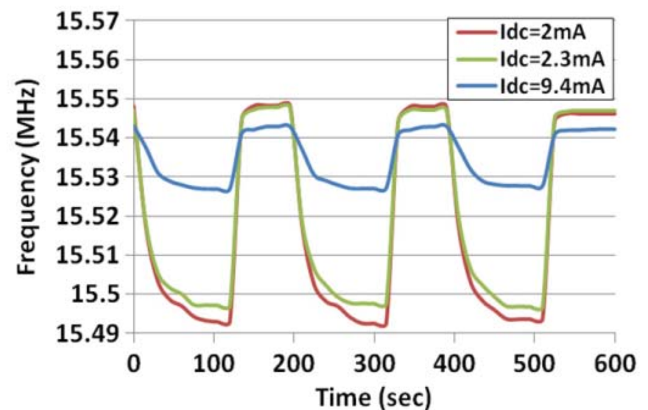


Fig. 11. Measured frequency response for the 15.5 MHz I-shaped resonator of Fig. 6 as a function of the cumulative exposure time. The three graphs show measurements taken at 3 different bias currents. Maximum frequency shift of 56 KHz (3600 ppm) is obtained at a bias current of 2 mA.

coated using the second presented method (releasing of the structure was done after polymer coating). As can be seen, upon exposure of the resonator to gasoline vapor, the resonance frequency reduces over time with a time constant of ~40sec. Again the resonant frequency is restored to its initial value almost instantaneously. It can be seen that a maximum frequency shift of ~2200ppm is achieved, which is more than 10 times the frequency shift obtained using the first coating procedure.

Figure 11 shows the measured resonance frequency of the structure of Fig. 6 biased at three different currents while going through 3 cycles of toluene absorption/desorption at room temperature. This device was coated using the third mentioned method (the same layer of photoresist used for patterning the device was used as the absorbent polymer layer). Upon exposure to the source, the resonance frequency decreases with a time constant of ~40 sec and again the resonance frequency moves back into its original position once the source is removed. As the resonator bias current and therefore its static temperature increases, the absorbed gas molecules move faster, and collide harder and more often. This leads to more of the gas molecules to break out and the gas absorption capacity to decrease. The observed maximum frequency shift of 3600ppm (55kHz) at a bias current of 2mA is almost double the highest values measured for the resonators coated through the second technique.

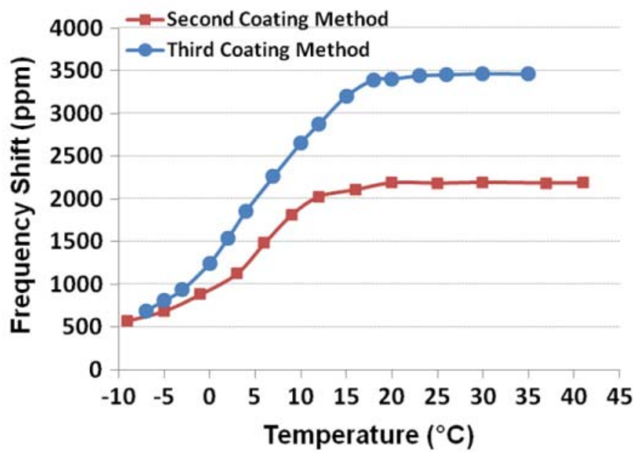


Fig. 12. Resonator frequency shift as a function of the temperature of the liquid source. The frequency shift increases with temperature as the organic vapor pressure increases. The increase is exponential at lower temperatures, until the sensor reaches saturation.

## V. Discussion

The mass sensitivity of the resonators can be theoretically calculated as follows:

$$f = \frac{1}{2\pi}\sqrt{\frac{k}{m}} \Rightarrow \frac{\partial f}{\partial m} = -\frac{f}{2m} \quad (1)$$

where $k$, $m$, and $f$ are the effective stiffness, effective mass and resonant frequency of the resonator respectively [21]. Knowing the dimensions and therefore the mass of the resonators, the mass of the absorbed organic molecules ($\partial m$) can be estimated from the measured frequency shifts. Assuming an approximate density of 720 kg/m$^3$ for the volatile organic compound, the volume and consequently the effective thickness of the absorbed organic compounds (assuming a uniform distribution over the top surface of the coated resonator) can be calculated. In the graph of Fig. 10, the observed maximum frequency shift of 2200 ppm (0.22%) is equivalent to an absorbed organic layer of ~40nm thick. Doing the same calculations for the graph shown in Fig.11, the observed maximum frequency shift of 3600 is equivalent to an absorbed organic layer of ~60nm thick.

In order to see how the sensor responds to different gas concentrations its frequency shift was measured while varying the temperature of the liquid source Fig. 12 shows the absolute value of the resonator frequency shift in ppm as a function of the temperature of the liquid source for both devices shown in Figures 4 and 6. As expected, at lower temperatures the lower organic vapor pressure leads to smaller frequency shifts. The shift increases sharply (almost exponentially) with temperature (as the vapor pressure increases exponentially with temperature). At about 5 °C, for the sensor shown in Fig. 4, the sensor response starts to saturate and stays constant for temperatures above ~15 °C. Saturation starts at about ~10 °C for the sensor shown in Fig. 6 and stays constant for temperatures above ~20 °C.

The vapor pressure of a liquid is an indication of a liquid's evaporation rate which can be calculated through the equation:

$$\ln P = -\frac{\Delta h}{RT} + C \ or \ P = e^{\left(-\frac{\Delta h}{RT} + C\right)}. \quad (2)$$

TABLE I
Summary of Measurement Results Obtained from Different Resonators at Different Bias Currents and the Calculated Equivalent Absorbed Toluene Thickness Values

| Dimensions (μm) (a/ b / H) (L/W) | Freq. (MHz) | Bias Current (mA) | Q. Factor | Freq. Shift (Hz) (ppm) | Equivalent Toluene Thickness (nm) |
|---|---|---|---|---|---|
| 31/ 22 / 5<br>36 / 3 | 15.5 | 9.4 | 4700 | -16100<br>1040 | 17 |
| | | 2.3 | 4500 | –50000<br>3220 | 55 |
| | | 2 | 4400 | –55100<br>3560 | 60 |
| 31 / 22 / 5<br>36 / 3 | 14.3 | 8 | 3900 | –15900<br>1110 | 19 |
| | | 6 | 3750 | –23600<br>1650 | 28 |
| | | 4 | 3600 | –39200<br>2740 | 47 |
| | | 2 | 3100 | –49800<br>3480 | 59 |
| 35 / 25 / 5<br>30 / 3 | 11.1 | 8 | 5260 | –12600<br>1135 | 19 |
| | | 6 | 5140 | –21200<br>1910 | 32 |
| | | 4 | 4900 | –32800<br>2955 | 49 |
| | | 2 | 4730 | –39100<br>3520 | 59 |

Here $\Delta h$ is the changes in enthalpy due to evaporation, $T$ is the temperature, $R$ is the mass specific gas constant, $P$ is the liquid vapor pressure and C is a constant. This equation, known as the Clausius–Clapeyron relationship shows that vapor pressure increases exponentially with temperature [24]. Therefore, the vapor pressure of liquid toluene versus its temperature has an exponential relationship [25]. The graphs depicted in Fig.12 follow this trend of showing an almost exponential change in frequency versus the temperature of the liquid source. This is due to the change of vapor pressure with the temperature of the liquid source.

Table 1 summarizes the measurement results obtained for different resonators coated using the third method presented. Since the devices have similar absorbent layers and the same structural thickness, the percentage shift in their resonant frequencies is similar. Based on the vapor pressure taken from [25], at a temperature of –10 °C, the minimum toluene concentration detected corresponds to ~4000 ppm whereas; assuming a minimum measurable frequency shift of 20Hz for the network analyzer, the minimum limit of detection (LOD) would be ~4.8 ppm.

## VI. Conclusion

High frequency thermally actuated in-plane silicon resonators were successfully used for detection of the presence of organic vapor in air. Three different coating methods were used and the sensitivity achieved using each method was compared.

The thickness of the deposited gas vapor on the surface of sensor was calculated according to the change in the resonant frequency of the resonator. The observed maximum frequency shift of 3600 ppm (55 kHz) was achieved when the same layer of photoresist used for patterning of the devices, was used as the absorbent coating layer for the resonators. This frequency shift is equivalent to an absorbed organic layer of ~60 nm thick in liquid form. Minimum LOD measurable is ~4.8 ppm. By using the last coating method, the response times have highly decreased, from ~4min to ~40 seconds.

## REFERENCES


[1] M. J. Fernandez, J. L. Fontecha, M. C. Horrillo, C. Vera, I. Obieta, and I. Bustero, "Surface acoustic wave gas sensors based on polyisobutylene and carbon nanotube composites," *J. Sensors Actuat. B*, vol. 156, no. 1, pp. 1–5, Aug. 2011.

[2] M. Penza, R. Rossi, M. Alvisi, M. A. Signore, G. Cassano, D. Dimaio, R. Pentassuglia, E. Piscopiello, E. Serra, and M. Falconieri, "Characterization of metal-modified and vertically-aligned carbon nanotube films for functionally enhanced gas sensor applications," *J. Thin Solid Film*, vol. 517, no. 22, pp. 6211–6216, Sep. 2009.

[3] H. Bai and G. Shi, "Gas sensors based on conducting polymer," *J. Sensors*, vol. 7, no. 3, pp. 267–307, 2007.

[4] S. A. Waghuley, S. M. Yenorkar, S. S. Yawale, and S. P. Yawale, "Application of chemically synthesized conducting polymer-polypyrrole as a carbon dioxide gas sensor," *J. Sensors Actuat. B: Chem.*, vol. 128, no. 2, pp. 366–373, Jan. 2008.

[5] Y. T. Li, H. C. Hao, M. C. Chen, T. H. Lin, P. H. Ku, C. M. Yang, K. T. Tang, and D. J. Yao, "Polymer-coated surface acoustic wave sensor array for low concentration $NH_3$ detection," in *Proc. IEEE NEMS Conf.*, Kaohsiung, Taiwan, Feb. 2011, pp. 333–337.

[6] L. A. Mashat, H. D. Tran, W. Wlodarski, R. B. Kaner, and K. Kalantar-zadeh, "Polypyrrole nanofiber surface acoustic wave gas sensors," *J. Sensors Actuat. B: Chem.*, vol. 134, no. 2, pp. 826–831, Sep. 2008.

[7] N. V. Quy, V. A. Minh, N. V. Luan, V. N. Hung, and N. V. Hieu, "Gas sensing properties at room temperature of a quartz crystal microbalance coated with ZnO nanorods," *J. Sensors Actuat. B: Chem.*, vol. 153, no. 1, pp. 188–193, Mar. 2011.

[8] M. Harbeck, D. Erbahar, I. Gurol, E. Musluoglu, V. Ahsen, and Z. Ozturk, "Phthalocyanines as sensitive coatings for QCM sensors: Comparison of gas and liquid sensing properties," *J. Sensors Actuat. B: Chem.*, vol. 155, no. 1, pp. 298–303, Jul. 2011.

[9] Y. Hwang, F. Gao, and R. N. Candler, "Porous silicon resonator for sensitive vapor detection," in *Proc. Solid State Sensors Actuat. Workshop*, 2010, pp. 150–153.

[10] M. C. Liu, C. L. Dai, C. Chan, and C. Wu, "Manufacture of a polyaniline nanofiber ammonia sensor integrated with a readout circuit using the CMOS-MEMS technique," *J. Sensors*, vol. 9, no. 2, pp. 869–880, 2009.

[11] O. Brand, "CMOS-based resonant sensors," in *Proc. IEEE Sensors Conf.*, Irvine, CA, Nov. 2005, pp. 129–132.

[12] L. Khine, J. M. Tsai, A. Heidari, and Y. J. Yoon, "Piezoelectric MEMS resonant gas sensor for defense applications," in *Proc. IEEE Defense Sci. Res. Conf.*, Singapore, Aug. 2011, pp. 1–3.

[13] G. Uma, M. Umapathy, L. B. Vidhya, M. Maya, T. Sophia, and K. Tamilarasi, "Design and analysis of resonant based gas sensor," in *Proc. IEEE Sens. Appl. Symp. Conf.*, Atlanta, GA, Feb. 2008, pp. 119–121.

[14] J. H. Seo and O. Brand, "High Q-Factor in-plane-mode resonant microsensor platform for gaseous/liquid environment," *J. Microelectromech. Syst.*, vol. 17, no. 2, pp. 483–493, Apr. 2008.

[15] A. Hajjam, J. C. Wilson, A. Rahafrooz, and S. Pourkamali, "Fabrication and characterization of thermally actuated micromechanical resonators for airborne particle mass sensing: II. Device fabrication and characterization," *J. Micromech. Microeng.*, vol. 20, no. 12, pp. 12501–12509, Dec. 2010.

[16] A. Rahafrooz and S. Pourkamali, "Fully micromechanical piezo-thermal oscillators," in *Proc. IEEE Int. Electron. Dev. Meeting*, San Francisco, CA, Dec. 2010, pp. 1–4.

[17] A. Pandey, G. C. Pandey, and P. B. Aswath, "Synthesis of polylactic acid–polyglycolic acid blends using microwave radiation," *J. Mech. Behavior Biomed. Mater.*, vol. 1, no. 3, pp. 227–233, Jul. 2008.

[18] A. Hajjam, J. Pandiyan, A. Rahafrooz, and S. Pourkamali, "MEMS resonant sensors for detection of gasoline vapor," in *Proc. IEEE Sensors Conf.*, Kona, HI, Nov. 2010, pp. 1538–1541.

[19] A. Hajjam, A. Logan, J. Pandiyan, and S. Pourkamali, "High frequency thermal-piezoresistive MEMS resonators for detection of organic gases," in *Proc. IEEE Int. Freq. Cont. Symp.*, San Francisco, CA, May 2011, pp. 1–5.

[20] A. Hajjam, A. Logan, and S. Pourkamali, "Fabrication and characterization of MEMS-based resonant organic gas sniffers," in *Proc. IEEE Sensors Conf.*, Limerick, Ireland, Oct. 2011, pp. 1–4.

[21] A. Hajjam, J. C. Wilson, A. Rahafrooz, and S. Pourkamali, "Detection and mass measurement of individual air-borne particles using high frequency micromechanical resonators," in *Proc. IEEE Sensors Conf.*, Kona, HI, Nov. 2010, pp. 2000–2004.

[22] G. K. Ho, K. Sundaresan, S. Pourkamali, and F. Ayazi, "Micromechanical IBARs: Tunable high-$Q$ resonators for temperature-compensated reference oscillators," *J. MEMS*, vol. 19, no. 3, pp. 503–515, Jun. 2010.

[23] A. Hajjam, J. C. Wilson, and S. Pourkamali, "Individual air-borne particle mass measurement using high frequency micromechanical resonators," *IEEE Sensors J.*, vol. 11, no. 11, pp. 2883–2890, Nov. 2011.

[24] M. Galleano, A. Boveris, and S. Puntarulo, "Understanding the Clausius-Clapeyron equation by employing an easily adaptable pressure cooker," *J. Chem. Edu.*, vol. 85, no. 2, pp. 276–278, Feb. 2008.

[25] S. Podhuvan. *Data Sheet, CRC Handbook of Chemistry and Physics* [Online]. Available: http://en.wikipedia.org/wiki/Toluene_(data_page)

**Arash Hajjam** (S'09) was born in Tehran, Iran. He received the B.S. degree in electrical engineering from the University of Tehran, Tehran, Iran, and the M.S. degree in bio-electrical engineering from the Iran University of Science and Technology, Tehran, in 2005 and 2008, respectively. He is currently pursuing the Ph.D. degree with the Department of Electrical and Computer Engineering, University of Denver, Denver, CO.

His current research interests include microelectromechanical system frequency references and resonant sensors.

Mr. Hajjam was a recipient of the Best Teaching Assistant Award from the School of Engineering and Computer Science, University of Denver, in 2009, the Best Student Paper Award from the ISCEE Electrical Engineering Conference in 2004, and the Professional Engineering License in the state of Colorado.

**Siavash Pourkamali** (S'02–M'06) received the B.S. degree in electrical engineering from the Sharif University of Technology, Tehran, Iran, and the M.S. and Ph.D. degrees in electrical engineering from the Georgia Institute of Technology, Atlanta, in 2001, 2004, and 2006, respectively.

He is currently an Assistant Professor with the Department of Electrical and Computer Engineering, University of Denver, Denver, CO. He holds several issued patents and pending patent applications in the areas of silicon micro/nanomechanical resonators and filters and nanofabrication technologies. His current research interests include integrated silicon-based microelectromechanical systems (MEMS) and microsystems, micromachining technologies, radio frequency MEMS resonators and filters, and nanomechanical resonant sensors.

Dr. Pourkamali was a recipient of the National Science Foundation CAREER Award in 2011, the University of Denver Best Junior Scholar Award in 2008, and the Georgia Tech Electrical and Computer Engineering Research Excellence Award in 2006. He was a Silver Medal winner in the 29th International Chemistry Olympiad in 1997.